Chem Soc Rev

Nanofabricated structures and microfluidic devices for bacteria: from techniques to biology

Journal:	*Chemical Society Reviews*
Manuscript ID:	CS-REV-06-2015-000514.R2
Article Type:	Tutorial Review
Date Submitted by the Author:	08-Sep-2015
Complete List of Authors:	Wu, Fabai; Delft University of Technology, Bionanoscience Dekker, Cees; TU Delft,

Nanofabricated structures and microfluidic devices for bacteria: from techniques to biology

Fabai Wu & Cees Dekker*

Delft University of Technology, Department of Bionanoscience, Kavli Institute of Nanoscience Delft, Lorentzweg 1, 2628CJ Delft, the Netherlands
*Correspondence can be addressed to Cees Dekker (c.dekker@tudelft.nl).

Abstract

Nanofabricated structures and microfluidic technologies are increasingly being used to study bacteria because of their precise spatial and temporal control. They have facilitated studying many long-standing questions regarding growth, chemotaxis and cell-fate switching, and opened up new areas such as probing the effect of boundary geometries on the subcellular structure and social behavior of bacteria. We review the use of nano/microfabricated structures that spatially separate bacteria for quantitative analyses and that provide topological constraints on their growth and chemical communications. These approaches are becoming modular and broadly applicable, and show a strong potential for dissecting the complex life of bacteria at various scales and engineering synthetic microbial societies.

Key learning points

1. Microfabricated structures can spatially isolate and separate bacteria for single-cell analyses, for drug discovery by cultivating natural species on chip, and for lineage tracking that reveal the rules governing cell growth, cell-fate decisions, and antibiotic resistance.

2. Microfluidic devices that separate bacteria with semipermeable materials allow dissecting the effect of chemical communication between bacteria that exchange metabolic compounds, signaling molecules, and antibiotic resistance.

3. Microhabitats can be fabricated with defined geometric features that constrain the growth patterns and social behavior of bacteria, leading to spatially structured populations that show rapid adaption to environmental stress.

4. Nanofabricated microchambers can be used to ‘sculpt’ bacteria into defined shapes and sizes for investigating the spatial adaption of their subcellular organization, such as how lipids sense curvature and how cell-division-related proteins form patterns to find symmetry axes and adapt to cell size.

5. The combination of microfluidics and synthetic genetic circuits allows for engineering synthetic microbial societies capable of organizing into defined structures and executing controllable functions.

Biology is a study of living matter in space and time. Nanotechnology provides tools that manipulate material in space and time with an exquisite amount of detail. With biology entering the quantitative era, there is an increasing demand for systematic and precise control over the spatial and temporal parameters in experiments. It therefore is becoming very appealing for biologists to pick up the toolkits from nanotechnology, such as nanofabricated structures and microfluidic technologies.

Much fundamental knowledge of biology is garnered through studying bacteria. While any organism exhibits an impressive amount of complexity, a bacterium is generally simpler than a eukaryote regarding its metabolic, signaling, and architectural networks. Hence, it is considerably easier to break down these networks into modules feasible for analysis and engineering. The versatile metabolic capacities shown in the bacterial kingdom represent a rich pool of resources, which have the potential of significantly contributing to solving the world's major issues such as food, energy, and medicine. In nature, bacteria play indispensible roles in ecosystems such as soil and human bodies. Meanwhile, they can be infectious agents that cause persistent medical problems. So far, our ability to cultivate bacteria, to harness their power as well as to extinguish them at will is far from satisfactory. This is largely due to our limited understanding of bacteria at many levels, from the orchestration of their inner structure to the rules governing their social behavior.

Nano- and microfabricated structures offer unique features to obtain previously unaccessible knowledge about bacteria. The spatial scales that can be manipulated by various lithography and etching techniques range from nanometer to centimeter size (Fig. 1A, 1B), that is, from the size of a protein cluster on the cell membrane to the size of a bacterial colony. The volume and pressure control provided by microfluidics enables rapid changes as well as long-term maintenance of defined chemical and physical environments for bacteria[1] (Fig. 1B). With these techniques, it is now possible to sort single bacterial cells from a soil or blood sample and designate them into individual compartments, where they can be separately cultivated, monitored and manipulated (Fig. 1C).

In this tutorial review, we introduce the application of nano- and microfabricated structures in bacteria by categorizing their functional purposes. We hope that such an overview will facilitate more microbiologists to pick up the experimental toolkits that are best suited for their applications (Fig. 1C) and that it will encourage further collaborations between microbiologists and nanoengineers. We start by introducing the major classes of fabrication techniques (Fig. 1A) and several essential elements that are in common use for applications in bacteria (Fig. 1B). Subsequently, we describe high-throughput applications realized by separating bacteria (Fig. 1C panel 1), which leads us to the subsequent long-term tracking of lineages (Fig. 1C, panel 2). Following spatial separation, the means to bring populations into chemical communication is introduced (Fig. 1C, panel 2). We then address the functional role of geometry at various spatial scales by presenting several global and local geometric features that illuminated the growth and adaptation of bacteria in space (Fig. 1C, panel 2). Zooming in further, we peek into the potential of cell-shaping techniques for studying subcellular organization (Fig. 1C, panel 3). Finally, we provide a brief outlook into the future opportunities and challenges of applying nanofabricated structures to studying bacteria.

1. Nano- and microfabrication of devices for bacteria

Chip devices used for studies of bacteria are in general a few centimeters across, a size suitable for manual handling and mounting onto platforms such as an optical microscope. The topological features on these devices can range widely, from the nanometer to centimeter scale. The division between nanofabrication and microfabrication is defined by the highest precision that is demanded for a device, roughly drawn at ~100nm, the resolution limit of most of the current optical approaches (see below). The two terms are, however, often interchanged since the key principles of fabrication are similar and the precision of a particular technique can vary according to equipment, recipes, and working conditions. The choice of fabrication technique depends not only on the precision, but also on several other factors such as the chemical and mechanical properties of the materials. Below, we introduce the basic principles of several major classes of fabrication techniques for readers who have a background outside of nanotechnology.

A nano/microstructure is typically fabricated through local modification of the chemical or physical properties of a flat substrate. The substrate is most commonly prepared through depositing a thin layer of organic materials, termed 'resist' onto a silicon surface through spin coating. The chemical property of the resist can be modified through patterned exposure to an energy source (Fig. 1A), which makes a local area either soluble or insoluble in a solvent. The photolithography technique patterns a surface two-dimensionally by transmitting (typically UV) light through a mask to the resist, which is fast and relatively inexpensive but requires a pre-patterned mask for each design. It is well suited for creating features with a resolution at the (sub)micrometer to millimeter range, such as the 200-μm wide microfluidic channel for studying biofilm formation in a constant flow stream[2] depicted in Fig. 1B (panel 2). Electron-beam lithography uses a local beam of electrons to draw a custom-designed pattern with, if desired, sub-10 nanometer resolution. It is required for patterning high-resolution features, such as the high-curvature corner of the triangular structure shown in Fig. 1B (panel 1), which was used as a mold to produce microchamber for shaping a bacterium[3]. After a quick chemical process that removes either the exposed or unexposed resist area, a device now has nano- or microscale features, which may be directly used or can be subject to further processing such as etching, surface modification, and other patterning steps. The structures created by the above methods can be directly transferred to another substrate through direct physical contact, which is used in soft lithography and nanoimprint technologies (Fig. 1A). Both methods uses organic materials that can be molded, hardened, and detached from the original stamp, such that one silicon chip fabricated by a nanoengineer can be used as a reusable mold for a biologist to produce hundreds of devices. In particular, the use of inexpensive, elastic materials such as PDMS (polydimethylsiloxane) and hydrogels in soft lithography[1] paved ways for many applications highlighted in this review. More recently, 3D micropatterning has been developed with two-photon polymerization and inkjet-based 3D printing (Fig. 1A). For studying bacteria, they are particularly useful in creating full confinement and complex topologies[4, 5]. Detailed descriptions of the above approaches can be found in ref[6].

Microfabricated structures can be used to accommodate and manipulate small volumes of fluids, a technology called microfluidics[1]. It can create physical and

chemical environments, such as a constant pressure[2] or constant nutrient replenishment[7], at a level that is inaccessible by conventional laboratory methods. One important function of microfluidics is to create defined chemical gradients, which has for example shed lights on the navigation of bacteria through chemotaxis, an application that will not be extensively discussed here given excellent recent reviews by Wessel *et al*[8] and Rusconi *et al*[9]. Many other applications have been developed. By modulating pressure, multichannel microfluidic devices have been used to switch medium rapidly (see review by Bennett *et al*, and references therein[10]). By mixing materials with different properties, a range of structures (microdroplets, microbubbles or microparticles) have been produced that are capable of encapsulating bacteria[1, 11, 12]. By stacking up two layers of PDMS channels, pneumatic vales were created that constrict one fluidic channel by applying pressure to the adjacent channel[13]. An ingenious development of using the opening and closing of such vales as binary inputs has led to large-scale complex manipulation using microfluidics[14] (Fig. 1B, panel 3). While this review focuses on simple nano- and microstructures for studies on bacteria, it is important to realize the strong engineering potential of the combination of complex microfluidic circuits and synthetic genetic circuits[15] (Fig. 1B, panel 4). Likewise, the combination of microstructures and microelectromechanical systems (MEMS) can be used to probe various physical properties of bacteria as well as their response to electromagnetic, optical and acoustic fields that can be generated locally on chip. One important recent advance is the studies on the structural origin of the electric conductivity of bacterial biofilms[16] (Fig. 1B, panel 5, also see review by Hol *et al*[17] and references therein).

2. Separated affairs

Rules in biology are often revealed by observations on individuals, and increasingly so, from statistical properties of data gathered from ensembles of such observations. Nano- and microfabricated devices are perfectly suited for separating individual cells or strains for manipulations and downstream analyses.

2.1 High-throughput platforms

Microstructures offer the capabilities to confine any small amounts of bacterial culture, encompassing volumes as small as one single cell. A large array composed of say 10^5 microchambers can for example be fabricated in an area of only a few square millimeters, spatially separating bacteria for subsequent manipulation and detection (Fig. 2A). This feature makes microstructures particularly effective as high-throughput platforms.

Diverse approaches have been developed to separate and encapsulate bacteria. The simplest forms are microchamber arrays from hydrogel, PDMS, or plastic, made mostly through soft lithography (Fig. 2A). These are often filled with bacteria by simple inoculation of bulk culture before getting sealed by hydrogel, a semipermeable membrane, or a piece of coverglass. These simple devices do not necessarily involve microfluidic circuits and can be readily adopted by regular microbiology laboratories, which can obtain microfabricated mold with the desired patterns commercially. Takeuchi *et al*[18], Renner *et al*[19], and Wu *et al*[3], for exampled, pipetted a small volume (~ 1 μl) of bacterial culture onto the surface patterned with microchambers, where bacteria were distributed into the chambers by capillary force after the surplus liquid was absorbed by agarose (Fig. 2A). This approach takes advantage of the large

number of microchambers: while bacterial cells enter the microchambers stochastically, the chambers with a desirable inoculation density can be selected afterwards through automated data analysis. The throughput for specific applications can be optimized by tuning the volume and density of the inoculated bacterial cultures as well as the size and distance of the microchambers. Such an approach has been used to study cellular mechanics, cell growth, cell division and subcellular organization, which are described in section 3.3.

The importance of physically separating bacteria into independent compartments is prominently exemplified by efforts to culture bacteria from natural microbial communities. This overcomes a long-standing issue that the majority of microorganisms are not cultivable on a conventional petri dish, as a 'winner-takes-all' competition leads to overgrowth of fast-growing bacterial species[20, 21]. Nichols *et al* developed a device called 'isolation chip' (or 'iChip'), which contains millimeter-sized through-holes for isolating bacteria from the natural environment and cultivating the species that were otherwise uncultivable[21, 22] (Fig. 2B). The iChip, made from (commercially manufactured) polyoxymethylene, was dipped into a liquid suspension of soil samples for encapsulation of single microbial cells into the through-holes, and then sandwiched by semipermeable polycarbonate membranes that allow chemical exchange of the enclosed colonies with the environment and with each other. The principles and advantages of semipermeable membranes are further discussed in section 2.3. This technique allows microbes from the soil sample to grow in separated spaces into millimeter-sized colonies (allowed by the chamber size) ready for downstream isolation and analysis. This technique provides a high-throughput platform for cultivating numerous new species that cannot be cultivated independently. In contrast to a ~1% successful cultivation using petri dishes, iChip was reported to recover up to 50% of the species[21], which is a spectacular advance. By screening the potential application of the metabolic compounds produced by the bacteria cultivated using iChip, Ling *et al* recently discovered a novel antibiotic that effectively kills persistent pathogens such as *Staphylococcus aureus* or *Mycobacterium tuberculosis,* so far without raising antibiotic resistance[22].

Independent culturing of bacteria in separated compartments allows high-throughput analyses of different strains and culturing conditions. A microfluidic device is most commonly constructed by covalently bonding a PDMS chip and a piece of glass, enabled by a simple oxygen plasma treatment (Fig. 2C). Using a PDMS-based microfluidic device as simple as smartly stacking up 96 parallel channels, Taniguchi *et al* injected individual bacterial strains into individual channels such that 96 different strains can be imaged simultaneously[23] (Fig. 2C). Here, each strain has a different gene fused to a yellow fluorescent protein gene. This approach facilitated the quantitative imaging of in total 1018 strains, leading to a quantification of the proteome and transcriptome in single cells with single-molecule sensitivity. Among other essential quantitative findings, they showed that a single cell's protein and mRNA copy numbers for any given gene are uncorrelated[23], contrasting the conventional perception that protein abundance scales with mRNA abundance. A key design principle of this study was to use semi-automation that reduces an unmanageably abundant sampling task to a feasible operation. In this case, in each experiment, all 96 microfluidic channels had to be manually connected to tubing for injection of bacteria, but it made downstream microscopy and analyses significantly more efficient. This indicates that, while microfluidics has the promise of complex

manipulations that potentially automate many processes, adopting a single feature at a time can already lead to an enormous advantage for a conventional microbiology lab.

Microfluidic devices can be much more versatile in single-cell analysis when integrating valve and droplet technologies, as they enable real-time compartmentalization and complex spatio-temporal control[1, 11-15]. Eun *et al* encapsulated single bacterial cells in agarose microparticles with volumes compatible with fluorescence-activated cell sorting (FACS)[11]. Such a platform enabled high-throughput screening and sorting of bacterial phenotypes in different chemical environments, such as the emergence of antibiotic resistance, for subsequent genotypic analysis[11]. Combining both pneumatic valves and microdroplets, Leung *et al* built a programmable, multiplex microfluidic device capable of precisely sorting, analyzing and cultivating microbes at single-cell level[12] (Fig. 2D). This device used peristaltic pumps to dispense a sub-femtoliter volume droplet of reagent or cell culture (from one of 8 inlets) into a flow stream, delivering it into one of the 95 storage chambers by using microvalves. Through an elegant control of flow rate, the droplet can either be docked at the entrance of the chambers for merging with another incoming droplet, or flushed away for downstream analyses. In addition, a cell-sorting module was integrated upstream through a feedback mechanism between optical detection and pumping, and an elution process is implemented downstream to recover the samples for off-chip analyses. The authors multi-purposed this droplet-based microfluidic device for various high-throughput applications including bacterial cell sorting and cultivation, taxonomic gene identification, and single-cell whole-genome sequencing[12].

2.2 Tracking lineage

In changing environments, a bacterial cell is constantly challenged with decisions to switch on and off the expression of genetic modules that define its metabolic capacity (e.g. through enzymes and transporters) or life style (e.g. through motility and biofilm formation). It is increasingly clear that the phenotypes of bacterial cells can vary even in the same environment, and can switch (seemingly) stochastically without environmental cues (see Norman *et al* and references therein[24]). Microstructures can offer spatial separation of populations and allow tracking of individual lineages over time within a steady chemical environment[7, 24-29] (Fig. 3A-D). Through inter- and intra-lineage comparisons of phenotypes made possible by this approach, biologists are starting to understand the origins and consequences of phenotypic variations (Fig. 3E). While bacteria have developed mechanisms to damp undesirable variations in order to reach homeostasis[28, 29] (Fig. 3F), other variations are now known to be beneficial as a bet-hedging strategy, that is, a stochastic switching of the phenotype for adaptation to different environments[24, 27, 30] (Fig. 3G, 3H). In addition, long-term tracking of lineage revealed the temporal control by genetic circuits responsible for oscillatory behaviors[26] (3I), and cell-fate decisions[24] (3G).

The main challenge for tracking a large number of lineages is that each single exponentially growing population rapidly expands to a size that is unsuitable for recording and analysis. An elegant alternative was the development of a microfluidic device dubbed the ‘mother machine’, which was composed of hundreds of line channels each sized to such a small width that they could only accommodate a single row of bacteria[7] (Fig 3A). These lines were connected to a large flow trench, which replenished the nutrients through diffusion as well as removed cells that exited the

line channels. As a result, the features of the mother cell that continuously remained at the end of a line channel and many newborn daughter cells could be recorded over time (Fig. 3F). The number of generations tracked per lineage was, however, limited due to the distance constrained by nutrient diffusion. Norman *et al* added a shallow side channel to enable feeding over a longer length scale for studying *B. subtilis*[24] (Fig. 3B); this feature is yet to be tested for gram-negative bacteria since they can potentially squeeze into the shallow side channels when crowded[31]. The use of agarose can allow for much more efficient diffusion of nutrients over a long distance (over 100 μm from the feeding channels)[25, 26] (Fig. 3C). However, agarose is less stiff and thus less effective in confining the cells strictly in a row[26] (Fig. 3I). Moffitt *et al* solved this issue by fabricating lines that were narrower (0.3-0.8 μm) but deeper (1-1.5 μm) than the width of the bacteria (~0.9 μm for *E. coli*), such that the bacteria slightly pushed the agarose aside during its growth along the linear tracks[25] (Fig. 3C). The efficient diffusion in agarose also entails an efficient exchange of signaling molecules and metabolites between lineages[25], which can be advantageous or disadvantageous depending on specific applications. Furthermore, a channel-length-independent delivery of nutrients and drugs can be achieved by vertical diffusion through a semi-permeable membrane[30], which in principle can allow for tracking of lineages for a large number of generations (Fig. 3D). Besides difference in stiffness, different materials also have different refractive indices and transparencies that can affect detection of bacteria in line structures using light microscopy[32].

Lineage tracking revealed the robustness of cell growth, division, and size control. Wang *et al* grew *E. coli* cells in the 'mother machine' for hundreds of generations, and found that the growth rate of *E. coli* cells was strikingly constant even in the mother cells that invariably inherited the old pole after each cell division[7] (Fig. 3B, 3F). While the inheritance of old pole had previously been proposed to lead to ageing as it inherit old cell wall material and misfolded proteins that aggregate at the polar regions, such ageing did not have a noticeable effect on the growth rate. By using the 'mother machine', the authors were able to maintain a steady-state growth of bacteria much better than previous studies using an agar pad (see Wang *et al*[7] and references therein). They showed that aging, while not affecting the growth rate, did lead to an increase in cell damage, which was indicated by the increasing rate of filamentous growth and cell death[7]. Using a similar experimental approach, Taheri-Araghi *et al* quantified the sizes of cells over many generations of growth and found that for both *E. coli* and *B. subtilis*, cells added a constant volume in between two division cycles, irrespective of their original sizes[29]. By abiding to this principle of constant cell-size extension, these bacteria reduce cell-size variations in steady-state growth and reach cell-size homeostasis. These findings were also reported for *Caulobacter crescentus* and *E. coli* by Campos *et al* using alternative microfluidic devices, where more cells were cultivated in each chamber, with lineage tracking aided by computer programs[28].

Lineage tracking has greatly elucidated the nature of environment-independent phenotypic variations and cell-fate switching. In a fast-growing culture, a small subpopulation of cells at a slow-growing state was found to be responsible for bacterial persistence to antibiotic treatments, and a mutation in the gene *hipA* increased the fraction of slow-growing cells significantly enhanced persistence[30] (Fig. 3D, 3H). Recently, another study showed that persistence could also be caused by an infrequent pulsing in the expression pattern of the proteins (KatG in *Mycobacterium smegmatis*) that are responsible for activating the antibiotics (INH), unrelated to

growth rate[27]. The authors proposed that stochastic switching of phenotype can be a universal strategy that enables adaptation to a broad spectrum of stress types, in addition to the costly sensing systems that respond to specific types of stress[27]. Although often stochastic switching of phenotype can be understood through the fluctuations inherent to the chemical environment inside of the cells[23], recent studies start to show that pulsing can be a regulatory feature hardwired in the genetic circuits (see review by Levine et al[33]). Norman et al studied the switching between the motile and chained states in *B. subtilis*, and found that although the emergence of the chained, multicellular state was infrequent, the time spent at the state was tightly controlled[24] (Fig. 3C, 3I).

2.3 Physical separation and chemical communication

Bacteria are social creatures. They communicate through secreting and sensing signaling molecules, cooperate to endure stress, and benefit from each other's unique metabolic capacity. They also combat for resources, and prey on one another. A great challenge in dissecting the social interactions between bacteria in bulk is to distinguish whether they are of a chemical or physical nature. Microstructures, when implemented with elements such as semipermeable membranes, hydrogel, and nanoslits, can be used to physically separate bacterial species or lineages while allowing chemical communications between them (see schematics in Fig. 4).

Members of a natural bacterial community often exhibit inter-dependent metabolic activities, that is, the growth of one species relies on metabolites secreted by another species. Thus, for example, the chemical exchange enabled by co-culturing process based on iChip (introduced in section 2.1) facilitated culturing of uncultivable species[21]. However, the complexity of metabolic exchange processes has only started to be dissected. Kim *et al* constructed a microfluidic device where 3 bacterial species were inoculated into spatially separated microwells, which were all connected to the same channel that mediates chemical communications[20] (Fig. 4A). These 3 species were respectively responsible for supplying the nitrogen source, carbon source, and for degrading antibiotics. They found that these species coexisted well with a finite inter-chamber distance, while the community collapsed either without any physical separation or with distances too large for the resources to be shared through diffusion[20]. Thus, the authors demonstrated that dynamic microbial communities should be understood in the context of spatial structures, which enable spatially separated growth and dictate the diffusivity of metabolic compounds. Recently developed 3D-printing of hydrogel structures provided even more versatile platforms to enclose and spatially organize multiple populations of bacteria for engineering of bacterial communities[5].

Bacteria make collective decisions through quorum sensing. Quorum sensing was discovered as a cell-density-dependent signaling behavior. By confining single bacteria in small hydrogel chambers that were chemically isolated, quorum response was triggered by accumulated quorum-sensing molecules within the chambers despite the low cell density[34, 35]. These experiments underlined the importance of understanding chemical communications within the context of spatial structures. Flickinger *et al* used hydrogels to physically separate bacterial biofilms and found that quorum sensing through the hydrogel chamber walls stimulated cell growth within the biofilms (Fig. 4B)[36]. The well-understood circuit responsible for quorum sensing was successfully applied to engineer synchronous cell behaviors. Prindle *et al*

constructed liquid crystal display like arrays of microchambers hosting independently growing bacterial colonies that detect arsenic[37]. They coupled the behavior within the bacterial colony through quorum sensing, which is then coupled between physically separated colonies through rapid gas-phase redox signaling that penetrates through the PDMS material. These bacteria synchronized their frequency of fluorescence oscillations over a large scale, showing the potential for constructing low-cost genetic biosensors[37].

Bacteria were found to mark territory through signaling without physical interactions. Van Vliet *et al* harvested bacteria from the same exponentially growing culture in a shaking tube and separately inoculated them into inlets at distant ends of two separate centimeter-long habitats, each containing many chambers that were mutually connected by thin corridors[38] (Fig. 4C). These two parallel habitats were connected through nanoslits that are 200 nm in height, too small for *E. coli* bacteria to swim through, but large enough to allow for chemical coupling. As shown in fig. 4C, the traveling front of one population (indicated in red) stopped progressing forward after it met the travelling front of the other population (labeled in green). Thus, this study elegantly demonstrated that the population fronts collided upon chemical communications alone without physical interactions[38].

3. Decoding geometries

Bacteria live in a world of structured environments. Nano- and microfabrication can achieve systematic control over the global as well as local topological features of the microenvironment, and thus can unravel the effects of the boundary geometry for bacterial population and even at the level of subcellular organization.

3.1 Populating a topological space

The topological features of bacteria's natural habitats influence the diffusivity of signals, nutrients, and metabolic waste, which are essential triggers of growth, attachment, and motility – behaviors that are in turn constrained by space. Hence, it is essential to understand the physiology and behavior of bacteria in the context of their spatial environment (Fig. 5).

Discreteness and heterogeneity are prominent features that distinguish the natural habitats of bacteria from well-mixed liquid cultures in the laboratory. Various forms of microhabitats have been fabricated to explore the effects of spatial heterogeneity on the ecological and evolutionary properties of bacterial populations. Park *et al* loaded *E. coli* cells into a microfabricated maze, where instead of dispersing throughout, bacteria formed travelling waves that nucleated dense populations into several dead ends within the maze[39] (Fig. 5A). This self-organized clustering phenomenon was further demonstrated in a more defined structure, and was found to be induced by the sensing of self-secreted amino acids by chemotactic receptors[39]. The authors thus showed that chemotaxis is not only employed by the cells to sense the gradient of exogenous nutrients as commonly understood, but also utilized to gather individuals to collectively seek for e.g. microcavities, a strategy that is likely beneficial for surviving nutrient deprivation[39]. Constructing a linear array of microhabitat patches connected by thin corridors, Keymer *et al* observed the formation of a metapopulation, that is, subpopulations coexisting in different patches and interacting through local extinction and colonization[40] (Fig. 5B). They further

showed that if nutrients and oxygen were supplied heterogeneously throughout the MHPs, such a metapopulation showed a rapid invasion from the high-resource areas to low-resource areas, revealing that the emergence of heterogeneous population structures facilitated by structured space can benefit adaptation[40]. The adaptive advantage of a metapopulation in a structured environment was further exemplified by a report of an accelerated emergence of antibiotic resistance in a large hexagonal device composed of 1200 hexagonal wells that were interconnected through corridors[41].

Local geometric features can affect the population structure at the global scale. Corridors between ecological niches, for example, can constrain the connectivity between these niches, both chemically and physically (Fig. 5C). Hol *et al* constructed a simple artificial ecosystem with a narrow corridor 100 μm in length connecting two large habitats that were both constantly replenished with nutrient (Losogeny broth medium) but only one of the two with an antibiotic kanamycin at a lethal concentration[42] (Fig. 5D). The corridor created a diffusion barrier that renders a steep concentration gradient at the interface between the two habitats, where bacteria combatted to survive under antibiotic stress. The authors found that a dense population of bacteria from the antibiotic-free zone was able to invade and colonize the antibiotic zone within several hours. Here, a sufficiently high density of the invading population was critical. As genetic mutations were not found at least in the first 29 hours after invasion, the authors provided evidence that the phenotypic adaptation responsible for the initial niche invasion can facilitate establishing a sizeable population as basis for the emergence of heritable genetic change[42].

Corridors also interfere with the behavior of swimming bacteria through physical collisions, where their geometric features can affect population-scale distributions. As shown in Fig. 5E, Galajda *et al* used a series of funnel walls that bias the destination of otherwise randomly moving *E. coli* towards one side of the device[43] (for follow-up applications of funnels, see review by Rusconi *et al* and references therein[9]).

3.2 Crowded and confined

At a critical scale where space becomes the constraining factor for the colonization by bacteria, the physical interactions between bacteria and the spatial boundary of the environment start to play an important role. Such a scenario occurs in the overgrowth with high-nutrient conditions, in the formation of biofilms, or by the self-organized clustering into tiny cavities that was mentioned above. How do bacteria organize themselves in these various forms of super-structures? Cho *et al* inoculated rod-shape *E. coli* cells in chambers with various distinct shapes, which were connected to fluidic channels that replenished nutrients and flushed away escaped cells[44]. In these chambers, bacteria showed orientation, growth and collective motion according to the shapes of the chambers and their locations within the chambers[44] (Fig. 5F). The authors used computer simulations to show that such self-organization phenomena can be explained by the combined effect of cell shape and mechanical forces between cells. Moreover, the resulting cell arrangements can decrease the mechanical stress induced by cell growth and promote efficient diffusion of nutrients[44]. Bacteria find solutions to crowding not only through minimizing mechanical stress, but also through maximizing attachment to local surface structures. This was exemplified by the spontaneous ordering of bacterial cells within periodically arranged nanoposts[45] (see Hol *et al* for more examples of surface adhesion[17]). The effect of crowding on the

physiology of bacteria is largely unclear. In a first study, Connell *et al* used hydrogel structures polymerized through multiphoton lithography to trap bacteria, and found that bacteria at high densities showed a much higher tolerance to the antibiotic gentamycin[4].

Invading new territories is another solution to local crowding that can tremendously benefit the survival of a population or a species. Männik *et al* used nanofabrication to systematically decrease the corridor between a patch that was highly populated by bacteria and an empty patch replenished with nutrients. For wide corridors, the bacteria would, not surprisingly, swim to the well-resourced empty patch. For very small corridors, however, they found a surprising effect: Here, rod-shape *E. coli*, a gram-negative bacterial species, was able to squeeze itself through corridors (made as slits in the silicon material) that were much narrower than their natural diameter of ~1 μm and subsequently propagate by growth[31] (Fig. 5G). The ability for bacteria to penetrate dimensions smaller than their size appears to depend on the internal turgor and the stiffness of the cell wall, as gram-positive bacteria *Bacillus subtilis* did not manage to do so to the same extent[31]. *E. coli* cells were found to adopt pancake-like irregular shapes while squeezing through shallow channels that were made for imaging[31] (Fig. 5G). These cells, although large and irregular in shape, can still partition their cytosolic volumes and DNA content equally into daughter cells during cell division[46] (Fig. 5G). It is an intriguing question whether and how other machineries within the bacteria respond to changes in cell shape.

3.3 Cell-shape sculpting

Zooming in on the inner environment of a cell, the spatial organization of intracellular molecular networks is dictated by the shape and size of the cell boundary. While the general importance of cell shape in bacteria is increasingly appreciated, it has been difficult to systematically probe the effects of specific geometric features embedded in the cell shape. Microstructures can be used to impose a certain shape to single bacteria. The ability to manipulate the cell shape of bacteria using nanofabricated structures is now starting to unravel the interplay between cell boundary and the molecular networks therein[3, 18, 19, 31, 46, 47].

The use of microstructures to guide the growth of single bacteria was first elegantly demonstrated by Takeuchi *et al*[18]. As shown in Fig. 6A, single *E. coli* bacteria were inoculated into donut-shaped microwells several microns in depth made from agarose supplemented with nutrients and a division-inhibitor cephalexin. After several hours, the growth of the bacteria followed the curvature of the microwells, yielding filaments that curled up along the defined shape of the agarose walls. Interestingly, after being released from the chambers, the cells maintained the spiral shapes, and adopted various modes of swimming patterns depending on the helicity of their cell shapes. Cabeen *et al* found that the mode of growth imposed by the agarose wells was similar to the emergence of the crescent shape of *C. crecentus*, leading them to propose that it is the mechanical strain borne by the cytoskeleton crescentin filaments anisotropically alters the cell-wall-insertion kinetics to produce curved growth[47].

Realizing that spatial constraints can mechanically shape bacterial growth opened up a range of possibilities for tackling timely questions in cell biology (Fig. 6B). For example, proteins and lipids were found to localize to the cell poles of bacteria by sensing the negative curvature (see Weibel *et al* and references therein[19]), and

dynamic protein patterns self-organize to form spatial gradients along the long axis of the cell (see Wu *et al* and references therein[3]).

Renner *et al* generated cell-wall-less spheroplasts that were highly moldable[19]. Long filamentous bacteria were osmotically protected by sucrose and treated with lysozyme before inoculating into agarose chambers. Without a stiff cell wall, these spheroplasts easily adapted to the shapes of the elliptical chambers with different aspect ratios and polar curvatures (Fig. 6C). The author stained the cells with nonyl acridine orange (NAO), a fluorophore that has high affinity for anionic lipids such as cardiolipin, and found that the labeled lipid microdomains preferably localize at the cell membrane area with high negative curvature (Fig. 6C). Some proteins however had lost their dynamic localization patterns in these spheroplasts, suggesting that the experimental protocols were yet to be improved to maintain the viability of the cells.

Improving upon the above methods, Wu *et al* combined the confinement strategy using nanofabricated chambers with a milder treatment that alters the cell wall synthesis. In this way, the authors achieved 'sculpting' of live bacterial cells into defined shapes[3] (Fig. 6D). The rod-shaped *E. coli* cells were first spherolized in liquid medium by using the drug A22 that impedes the dynamics of bacterial actin MreB, which would otherwise guide the global cell-wall insertion pattern to maintain the rod shape. These cells were inoculated into PDMS microchambers, a much stiffer polymer than agarose, with various shapes and sizes, which were then sealed noncovalently by a layer of agarose containing nutrient, A22, and cephalexin. These cells adopted the shapes of the microchambers by adaptive growth, where the ability to grow indicated the viability[3] (Fig. 6D). The authors used these cells to study the spatial adaptation of the Min proteins, which form pole-to-pole oscillations in a regular rod-shape *E. coli* to inhibit the cell divisions at the poles, and as a result facilitate the division in the cell center. The oscillations are driven by a Turing-type reaction-diffusion mechanism. As shown in Fig. 6B, MinD proteins, in their ATP-bound form, cooperatively bind to the membrane, which subsequently are bound by MinE which then triggers their ATPase activity and unbind MinD from the membrane. Intriguingly, The MinD proteins sense the cell shapes and align their oscillation directions to the symmetry axes (Fig. 6D). In addition, the time-averaged MinD concentration gradients adapt to the cell size by scaling within a characteristic length range of 3-6 μm^3. These properties were proposed to be essential for the Min system to facilitate accurate selection of division axes in *E. coli* and other organisms. This method shall find future applications in understanding the interplay between cell shape and other subcellular structures such as protein clusters, cytoskeleton, and chromosomes.

4. Opportunities and challenges

The use of nanofabricated structures and microfluidics holds great promise for studying bacteria. Not only do they provide systematic and quantitative means for solving long-standing questions in topics such as growth, chemotaxis, and cell-fate switching, but they also open up new classes of studies such as investigating the roles of boundary geometry in subcellular organization, population dynamics and evolution. The examples described in this review, along with many other studies, have demonstrated approaches with strong modularity and transferability. For example, individual topological modules, such as line channels, corridors, and semipermeable membranes are broadly applicable for studies of many other phenomena in bacteria.

With this, studying bacteria using nanofabricated structures and microfluidics is growing out of its infancy.

Looking at emerging techniques, an increasing number of proof-of-principle studies indicate a broad application potential of simple methods that do not involve fluidic control, such as the 'iChip' (section 2.1) and the cell-shaping methods (section 3.3). These powerful single-purposed techniques will undoubtedly contribute to dissecting the bacterial world from the metabolic biodiversity of the natural microbial communities to the architectural complexity of a bacterial cell.

Versatile functions can be achieved by multiplex devices that combine microfluidics with MEMS, biophysical tools, and synthetic genetic circuits. They enable measuring many physical properties, such as electrical conductivity[16], as well as probing the effect of force on cellular structures such as chromosomes[48]. Exciting engineering opportunities lie ahead in the integration of the microfluidics-based circuits that control chemicals in space and time and the genetic circuits that control gene expression, quorum sensing, chemotaxis, and biofilm formation[15, 37, 49]. This will lead to building synthetic microbial societies that are capable of organizing into defined structures and execute controllable functions. From there, directed evolution is possible.

With the many opportunities that are not-at-all far fetched, also some challenges lie ahead. The integration of a new technology into a microbiology laboratory depends on whether it holds an absolute advantage over a conventional technique, and on whether the integration process is cost and labor friendly. For example, while microfluidics is ideal for the isolation of single-bacteria for sequencing, it currently does not hold a strong advantage over the encapsulation and sorting methods based on flow cytometry (FACS) that is commonly available in biology laboratories. The accessibility of nanofabricated structures and microfluidic technologies relies on their future commercialization and on collaborations between microbiologists and nanoengineers. Such technological integration is greatly stimulated by cheap materials and emerging fabrication techniques, such as paper-based microfluidics[50] and hydrogel-based 3D printing[5]. In addition, customizing downstream analytic tools is essential for microbiologists to successfully adopt microstructure-based studies for routine studies. For example, geometry-related studies would benefit from software developed for automatic recognition of cell shapes or population structures in microchambers.

We look forward to the exciting new biology that will emerge from the integration of nanofabricated structures into the studies of bacterial life.

Acknowledgements
We thank F. Hol, S. van Vliet, and Y. Caspi for their critical comments on the manuscript, J. Keymer, P. Galajda, and J. Männik for previous valuable discussions. This work was supported by the ERC Advanced Grant SynDiv (No. 669598), the Netherlands Organisation for Scientific Research (NWO/OCW) as part of the Frontiers of Nanoscience program, and NanoNextNL program 3B Nanomedicine.

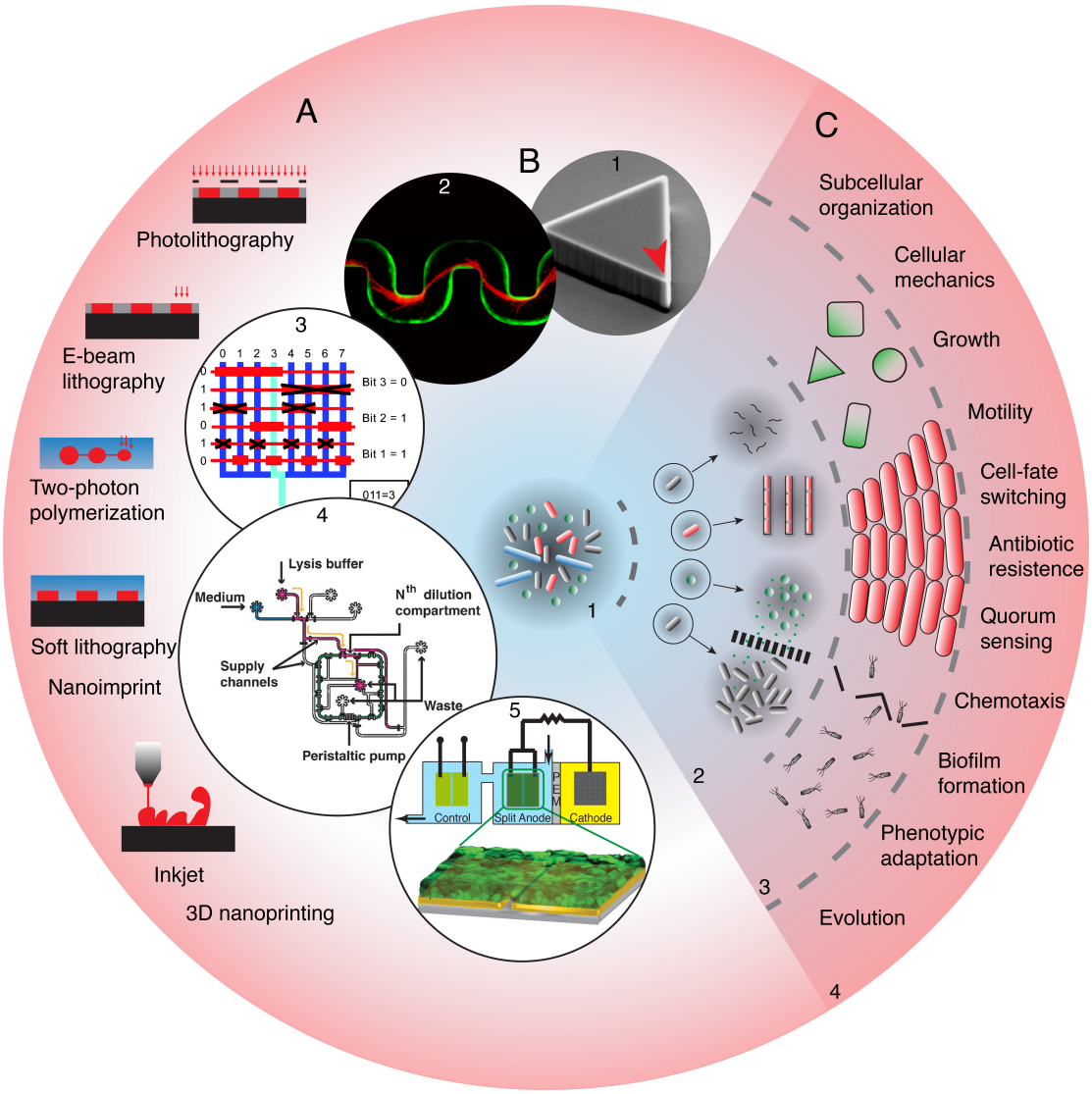

Figure 1. Nanofabricated structures and microfluidic devices for bacteria: from techniques to biology. **A.** Illustrations of basic nano- and microfabrication processes viewed at cross-sections (left outer circle). Black blocks indicate substrate (mostly silicon). Black lines in the first schematic indicate mask. Grey is spin-coated resist. Red shows the area modified by the lithography techniques. Blue indicates transparent polymeric material. **B.** Images in circles show nano- and microscale structures and their multiplex applications. From top to bottom: 1, a silicon structure with a triangle shape (side lengths 4.5 μm) nanofabricated through electron-beam lithography (electron-beam steps 20nm) and etching (red arrow indicates the sharp corner) [Adapted with permission from ref. 3]. 2, a 200-μm wide microfluidic channel (fabricated through optical lithography and soft lithography) with fluorescent bacteria forming a biofilm in a flow stream [Reprinted with permission from ref. 2]. 3, binary inputs defined by pneumatic pumps for large-scale integration of microfluidic devices. [Reprinted with permission from ref. 14]. 4. Schematics of a multiplex microfluidic device used for long-term monitoring of bacteria populations. [Reprinted with permission from ref. 15]. 5. A MEMS device used to measure conductive properties of bacterial biofilms. [Adapted with permission from ref. 16]. **C.** Various examples of biological applications in this review. The image illustrates 4 layers divided by dashed lines from left to right: 1, a bacteria community composed of different bacterial species; 2, microstructures spatially separate bacteria for DNA amplification and sequencing, lineage tracking, and chemical communication (from top to bottom); 3, adaptation of bacteria into nanofabricated structures that allow studying cell

shape, crowd control, and motility (from top to bottom); and 4, a range of biological questions highlighted in this review.

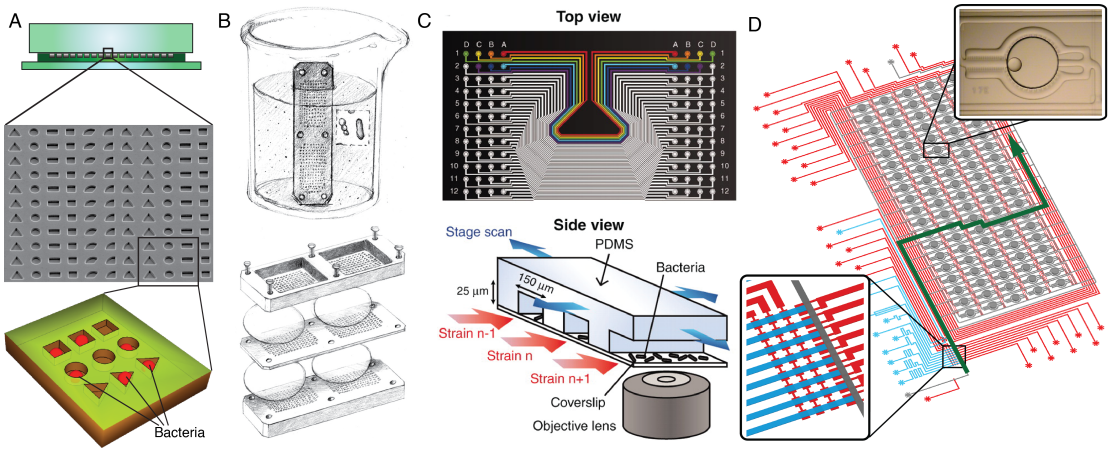

Figure 2. High-throughput devices made from nano/microfabricated structures. **A**. A simple device using PDMS microstructures of different shapes to confine single bacterial cells. Shown from top to bottom are a schematic of cross section of the agarose/PDMS/glass sandwich, a scanning electron microscopy image of the microstructures, and an illustration of bacteria in these microchambers. [Adapted with permission from ref. 3] **B**. Sketches of the 'iChip' used to capture single bacterial cells from a soil suspension (top) and the through-holes sandwiched by semipermeable membranes (bottom) for further cultivation. [Reprinted with permission from ref. 21]. This device enabled culturing of unculturable microbes and led to discovery of new antibiotics [ref. 22]. **C**. A microfluidic device with an array of microfluidic channels used for high-throughput quantification of the proteome and transcriptome of single bacteria through fluorescence imaging. [Reprinted with permission from ref. 23]. **D**. A programmable microfluidic device composed of peristaltic pumps (magnified at the bottom left) and droplets (magnified at top right) for enclosing single bacteria for cultivation and genome sequencing. The green arrow shows one possible flow path. [Adapted with permission from ref. 12].

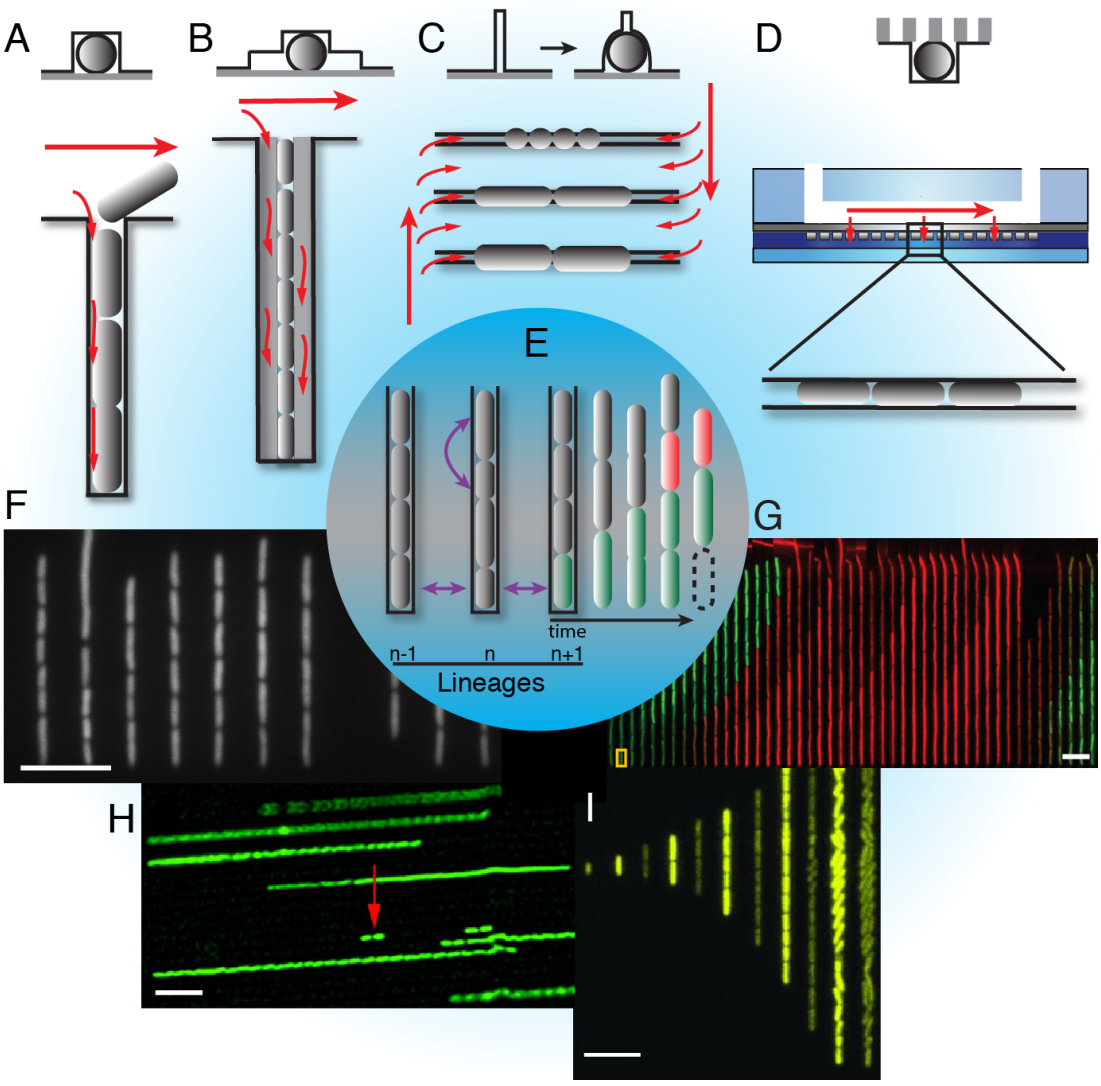

Figure 3. Line channels for lineage tracking. **A-D**, Schematics of various line-channel devices with different nutrient accessibility. In each panel: top is cross-section and bottom is top view). Large red arrows show the direction of the fluid flow; small red arrows show nutrients accessing the channels with cells. **E**. Illustration in the center: linear colonies in the line channels are used for inter-lineage (numbered n-1, n, n+1) and intra-lineage (e.g. in lineage n) comparisons (magenta arrows), and for long-term tracking allowing studies of cell-fate switching (from grey to red cell) and the mechanisms of growth (green), cell size control, and cell death (dashed rod). **F-I**, fluorescent images of cells growing in line channels. **F**. A snap shot of *E. coli* lineages growing in mother machine. [Reprinted with permission from ref. 7]. **G**. A kymograph of a *B. subtilis* lineage. Green, the motile state; red, the chained state; yellow box, time point of cell-fate switching. Time interval between frames is 10 minutes. [Reprinted with permission from ref. 24]. **H**, A snap shot of *E. coli* cells growing in line channels. The red arrow indicates two cells showing slow growth. [Reprinted with permission from ref. 30]. **I**, Time-lapse images showing Cyanobacteria *Synechococcus elongatus* with YFP expression under the promoter of *kaiBC* genes, which are involved in controlling circadian oscillations. Time interval between frames is 12 hours. [Reprinted with permission from ref. 26]. Scale bars in F-I are all 10 μm.

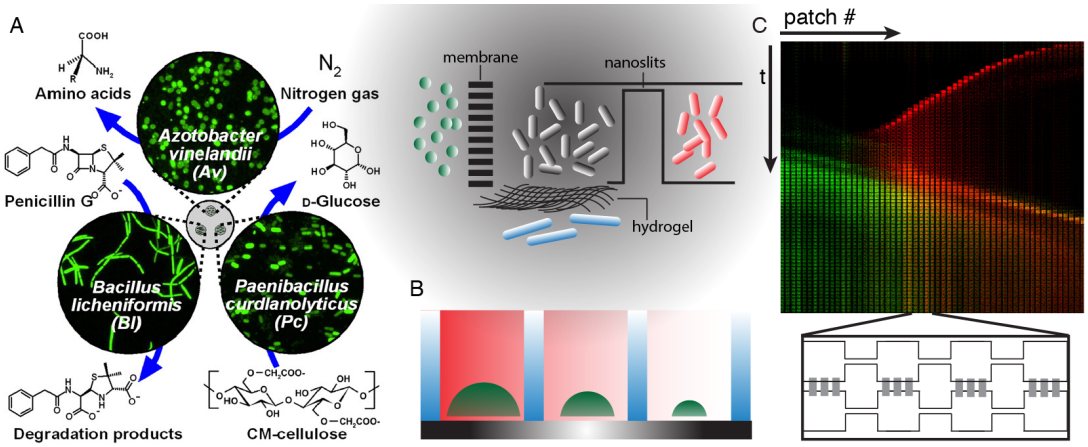

Figure 4. Chemical communication between physically separated bacterial populations in microstructures. Schematic in the top-middle shows bacteria spatially separated by a semipermeable membrane, hydrogel or nanoslits. **A**. Three bacterial species sharing metabolic products and penicillinase through a chemical chamber that mutually separates the bacteria through a cellulose membrane. [Reprinted with permission from ref. 20]. **B**. Hydrogel walls (blue) separating bacterial biofilms (green), which communicate through quorum sensing molecules HSL (red) that promote biofilm growth. [Modified from ref. 36]. **C**. Kymograph showing two populations of the same *E. coli* strain travelling in two parallel microhabitat patches that are chemically connected through 200-nm deep nanoslits (see bottom illustration, nanoslits in grey). The two populations enter from the left (green) and right (red), respectively, and influenced each other's propagation although they do not have physical contact. [Reprinted with permission from ref. 38].

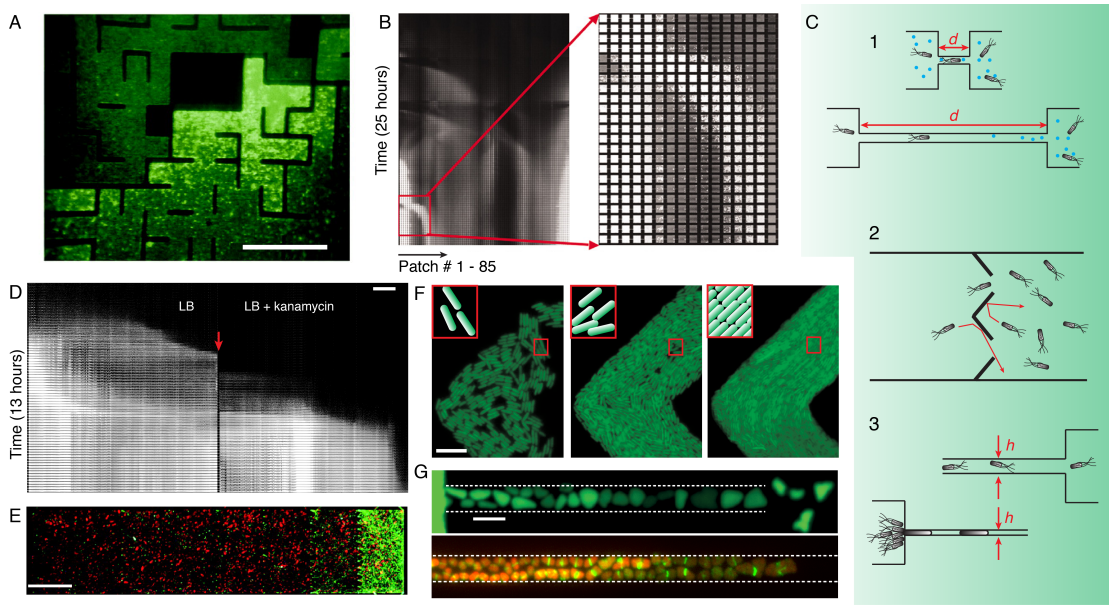

Figure 5. Effect of nanofabricated topological features on bacterial populations. **A**. Chemotactic *E. coli* bacteria (with green fluorescence) cluster at dead ends of nanofabricated mazes. Scale bar, 200 μm. [Reprinted with permission from ref. 39]. B. Temporal evolution of a bacterial metapopulation in 85 microhabitat patches connected through narrow corridors. [Reprinted with permission from ref. 40]. **C**. Illustrations showing how the geometries of the corridors between microhabitats affect the behavior of bacteria. 1. The length (*d*) of the corridors affects the diffusivity of the nutrients, antibiotics, and signaling molecules (depicted by the blue circles) between two chambers, thus reducing chemical communication (as in D). 2. Funnels concentrate bacteria to one side (as in E). Red indicates the paths of the swimming bacteria before and after collision onto the funnel walls. 3. Decreasing the width (*h*) of the corridors to smaller than the cells stop them from swimming through (top), but instead cause the gram-negative bacteria to grow and squeeze through (bottom) (as in G). **D**. A dense population of fluorescent *E. coli* bacteria invading a new territory with a lethal concentration of kanamycin. The corridor between the left and right device, indicated by the red arrow, is 100 μm long and 5 μm wide. Scale bar, 1 mm. [Reprinted with permission from ref. 42]. **E**. Motile *E. coli* (in green) are concentrated by a series of funnels (shown in the illustration at the right) to the rightmost chamber, while the non-motile *E. coli* (in red) homogeneously distribute throughout the device. Scale bar, 200 μm. [Reprinted with permission from ref. 43]. **F**. With increasing cell density, bacteria self-organize to orient themselves according to their location in the chambers with a defined geometry. Time intervals between frames are 2 hours and 22 hours, respectively. Top left corners zoom in on the bacteria in the red rectangles indicated at the right. Scale bar, 10 μm. [Adapted with permission from ref. 44]. **G**. *E. coli* bacteria squeeze through channels 300 nm in depth and changed their lateral dimensions and shapes (top view). The boundaries of the shallow channels are indicated by dashed lines. Top panel shows cytosolic fluorescence [Reprinted with permission from ref. 31]; bottom panel shows chromosome (red) and division machinery (green) [Image courtesy of Jaan Männik (ref. 46)]. Scale bar, 5 μm.

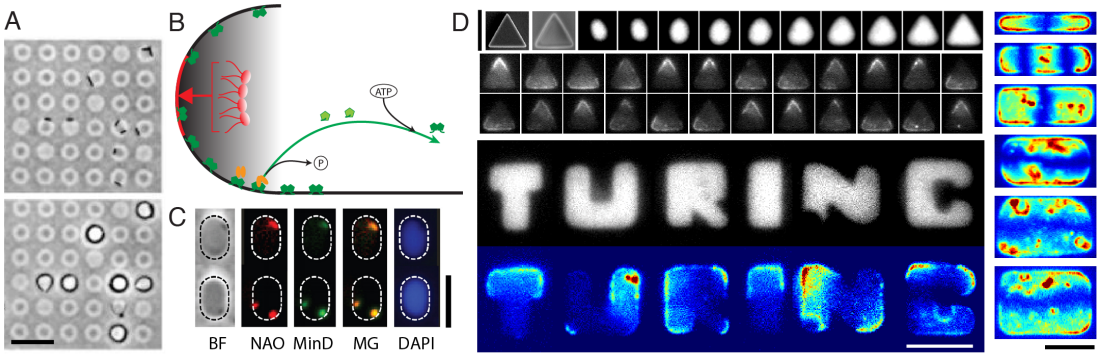

Figure 6. Cell shaping techniques used to study subcellular organization. **A**. Rod-shape *E. coli* (top) grow into filaments (bottom) as they adapt to the curvature of the donut-shaped agarose chambers. Scale bar, 20 μm. [Reprinted with permission from ref. 18]. **B**. Schematic that illustrates the mechanisms responsible for the polar localization of proteins and lipids. The curved line at the left depicts the bacterial cell pole and the flat line at the bottom depicts the non-polar membrane. Anionic lipids (shown in red) preferably form microdomains that have an intrinsic curvature and thus prefers the negatively curved cell pole. MinD proteins (in green) oscillate between the two cell poles through a reaction-diffusion mechanism. When MinE (orange) binds to the membrane-bound MinD (green), it triggers the ATPase activity of MinD and unbinds the latter from the membrane. MinD.ADP diffuse in the cytosol while undergoing an ADP-ATP exchange cycle and relocate at a distance (green arrow). **C**. Spheroplasts of *E. coli* cells prepared using lysozyme adopt the shapes of microchambers with an elliptic shape. BF, bright field; NAO, nonyl acridine orange signal; MinD, YFP-MinD signal; MG, merge; DAPI, a DNA stain. Scale bar, 5 μm. [Reprinted with permission from ref. 19]. **D**. 'Cell-sculpting' method used to shape bacteria into defined shapes, in which Min proteins oscillate. Top left: SEM images of the silicon mode and the PDMS structure followed by time-lapse fluorescence images of slow cell growth into a triangle shape in the PDMS structure (top row), followed by time-lapse fluorescence images of GFP-MinD oscillations in the shaped cells. Bottom left: A snapshot of cytosolic fluorescence (in grey scale) and GFP-MinD fluorescence (in color map) of six individual bacteria that were shaped into the letters 'TURING'. Right: standard-deviation images of GFP-MinD patterns in rectangular 9 μm long cells with cell widths increasing from 1 to 6 μm. Color maps: values from high to low: red-yellow-green-blue. Scale bars are all 5 μm. [Reprinted with permission from ref. 3].

References

1. G. M. Whitesides, *Nature*, 2006, **442**, 368-373.
2. K. Drescher, Y. Shen, B. L. Bassler and H. A. Stone, *Proc Natl Acad Sci USA*, 2013, **110**, 4345-4350.
3. F. Wu, B. van Schie, J. E. Keymer and C. Dekker, *Nat Nanotechnol*, 2015, **10**, 719-726.
4. J. L. Connell, A. K. Wessel, M. R. Parsek, A. D. Ellington, M. Whiteley and J. B. Shear, *mBio*, 2010, **1**.
5. J. L. Connell, E. T. Ritschdorff, M. Whiteley and J. B. Shear, *Proc Natl Acad Sci USA*, 2013, **110**, 18380-18385.
6. M. J. Madou, *Fundamentals of Microfabrication and Nanotechnology*, 3 edn., CRC Press, 2011.
7. P. Wang, L. Robert, J. Pelletier, W. L. Dang, F. Taddei, A. Wright and S. Jun, *Curr Biol*, 2010, **20**, 1099-1103.

8. A. K. Wessel, L. Hmelo, M. R. Parsek and M. Whiteley, *Nat Rev Micro*, 2013, **11**, 337-348.
9. R. Rusconi, M. Garren and R. Stocker, *Annu. Rev. Biophys.*, 2014, **43**, 65-91.
10. M. R. Bennett and J. Hasty, *Nat Rev Genet*, 2009, **10**, 628-638.
11. Y.-J. Eun, A. S. Utada, M. F. Copeland, S. Takeuchi and D. B. Weibel, *ACS Chem Biol*, 2011, **6**, 260-266.
12. K. Leung, H. Zahn, T. Leaver, K. M. Konwar, N. W. Hanson, A. P. Pagé, C.-C. Lo, P. S. Chain, S. J. Hallam and C. L. Hansen, *Proc Natl Acad Sci USA*, 2012, **109**, 7665-7670.
13. M. A. Unger, H.-P. Chou, T. Thorsen, A. Scherer and S. R. Quake, *Science*, 2000, **288**, 113-116.
14. T. Thorsen, S. J. Maerkl and S. R. Quake, *Science*, 2002, **298**, 580-584.
15. F. K. Balagaddé, L. You, C. L. Hansen, F. H. Arnold and S. R. Quake, *Science*, 2005, **309**, 137-140.
16. N. S. Malvankar, M. Vargas, K. P. Nevin, A. E. Franks, C. Leang, B.-C. Kim, K. Inoue, T. Mester, S. F. Covalla, J. P. Johnson, V. M. Rotello, M. T. Tuominen and D. R. Lovley, *Nat Nanotechnol*, 2011, **6**, 573-579.
17. F. J. H. Hol and C. Dekker, *Science*, 2014, **346**.
18. S. Takeuchi, W. R. DiLuzio, D. B. Weibel and G. M. Whitesides, *Nano Letters*, 2005, **5**, 1819-1823.
19. L. D. Renner and D. B. Weibel, *Proc Natl Acad Sci USA*, 2011, **108**, 6264-6269.
20. H. J. Kim, J. Q. Boedicker, J. W. Choi and R. F. Ismagilov, *Proc Natl Acad Sci USA*, 2008, **105**, 18188-18193.
21. D. Nichols, N. Cahoon, E. M. Trakhtenberg, L. Pham, A. Mehta, A. Belanger, T. Kanigan, K. Lewis and S. S. Epstein, *Appl Environ Microbiol*, 2010, **76**, 2445-2450.
22. L. L. Ling, T. Schneider, A. J. Peoples, A. L. Spoering, I. Engels, B. P. Conlon, A. Mueller, T. F. Schaberle, D. E. Hughes, S. Epstein, M. Jones, L. Lazarides, V. A. Steadman, D. R. Cohen, C. R. Felix, K. A. Fetterman, W. P. Millett, A. G. Nitti, A. M. Zullo, C. Chen and K. Lewis, *Nature*, 2015, **517**, 455-459.
23. Y. Taniguchi, P. J. Choi, G.-W. Li, H. Chen, M. Babu, J. Hearn, A. Emili and X. S. Xie, *Science*, 2010, **329**, 533-538.
24. T. M. Norman, N. D. Lord, J. Paulsson and R. Losick, *Nature*, 2013, **503**, 481-486.
25. J. R. Moffitt, J. B. Lee and P. Cluzel, *Lab Chip*, 2012, **12**, 1487-1494.
26. S.-W. Teng, S. Mukherji, J. R. Moffitt, S. de Buyl and E. K. O'Shea, *Science*, 2013, **340**, 737-740.
27. Y. Wakamoto, N. Dhar, R. Chait, K. Schneider, F. Signorino-Gelo, S. Leibler and J. D. McKinney, *Science*, 2013, **339**, 91-95.
28. M. Campos, Ivan V. Surovtsev, S. Kato, A. Paintdakhi, B. Beltran, Sarah E. Ebmeier and C. Jacobs-Wagner, *Cell*, 2014, **159**, 1433-1446.
29. S. Taheri-Araghi, S. Bradde, John T. Sauls, Norbert S. Hill, Petra A. Levin, J. Paulsson, M. Vergassola and S. Jun, *Curr Biol*, 2015, **25**, 385-391.
30. N. Q. Balaban, J. Merrin, R. Chait, L. Kowalik and S. Leibler, *Science*, 2004, **305**, 1622-1625.
31. J. Männik, R. Driessen, P. Galajda, J. E. Keymer and C. Dekker, *Proc Natl Acad Sci USA*, 2009, **106**, 14861-14866.

32. F. Wu, E. van Rijn, B. G. C. van Schie, J. E. Keymer and C. Dekker, *Front Microbiol*, 2015, **6**, 607.
33. J. H. Levine, Y. Lin and M. B. Elowitz, *Science*, 2013, **342**, 1193-1200.
34. J. Q. Boedicker, M. E. Vincent and R. F. Ismagilov, *Angew Chem Int Ed*, 2009, **48**, 5908-5911.
35. E. C. Carnes, D. M. Lopez, N. P. Donegan, A. Cheung, H. Gresham, G. S. Timmins and C. J. Brinker, *Nat Chem Biol*, 2010, **6**, 41-45.
36. S. T. Flickinger, M. F. Copeland, E. M. Downes, A. T. Braasch, H. H. Tuson, Y.-J. Eun and D. B. Weibel, *J. Amer. Chem. Soc.*, 2011, **133**, 5966-5975.
37. A. Prindle, P. Samayoa, I. Razinkov, T. Danino, L. S. Tsimring and J. Hasty, *Nature*, 2012, **481**, 39-44.
38. S. van Vliet, F. Hol, T. Weenink, P. Galajda and J. Keymer, *BMC Microbiology*, 2014, **14**, 116.
39. S. Park, P. M. Wolanin, E. A. Yuzbashyan, H. Lin, N. C. Darnton, J. B. Stock, P. Silberzan and R. Austin, *Proc Natl Acad Sci USA*, 2003, **100**, 13910-13915.
40. J. E. Keymer, P. Galajda, C. Muldoon, S. Park and R. H. Austin, *Proc Natl Acad Sci USA*, 2006, **103**, 17290-17295.
41. Q. Zhang, G. Lambert, D. Liao, H. Kim, K. Robin, C.-k. Tung, N. Pourmand and R. H. Austin, *Science*, 2011, **333**, 1764-1767.
42. F. J. H. Hol, B. Hubert, C. Dekker and J. E. Keymer, *The ISME Journal*, 2015, **Advance online publication**, doi:10.1038/ismej.2015.107.
43. P. Galajda, J. Keymer, P. Chaikin and R. Austin, *J Bacteriol*, 2007, **189**, 8704-8707.
44. H. Cho, H. Jönsson, K. Campbell, P. Melke, J. W. Williams, B. Jedynak, A. M. Stevens, A. Groisman and A. Levchenko, *PLoS Biol*, 2007, **5**, e302.
45. A. I. Hochbaum and J. Aizenberg, *Nano Letters*, 2010, **10**, 3717-3721.
46. J. Männik, F. Wu, F. J. H. Hol, P. Bisicchia, D. J. Sherratt, J. E. Keymer and C. Dekker, *Proc Natl Acad Sci USA*, 2012, **109**, 6957-6962.
47. M. T. Cabeen, G. Charbon, W. Vollmer, P. Born, N. Ausmees, D. B. Weibel and C. Jacobs-Wagner, *The EMBO Journal*, 2009, **28**, 1208-1219.
48. J. Pelletier, K. Halvorsen, B.-Y. Ha, R. Paparcone, S. J. Sandler, C. L. Woldringh, W. P. Wong and S. Jun, *Proc Natl Acad Sci USA*, 2012, **109**, E2649-E2656.
49. S. H. Hong, M. Hegde, J. Kim, X. Wang, A. Jayaraman and T. K. Wood, *Nat Commun*, 2012, **3**, 613.
50. A. W. Martinez, S. T. Phillips and G. M. Whitesides, *Proc Natl Acad Sci USA*, 2008, **105**, 19606-19611.